

Mapping Soil Moisture as an Indicator of Wildfire Risk Using Landsat 8 Images in Sri Lanna National Park, Northern Thailand

Kansuma Burapapol¹ & Ryota Nagasawa²

¹ The United Graduate School of Agricultural Sciences, Tottori University, Tottori, Japan

² Faculty of Agriculture, Tottori University, Tottori, Japan

Correspondence: Kansuma Burapapol, The United Graduate School of Agricultural Sciences, Tottori University, 4-101 Koyama Minami, Tottori 680-8553, Japan. E-mail: kansuma.bu@gmail.com

Received: July 7, 2016

Accepted: August 10, 2016

Online Published: September 15, 2016

doi:10.5539/jas.v8n10p107

URL: <http://dx.doi.org/10.5539/jas.v8n10p107>

Abstract

Severely dry climate plays an important role in the occurrence of wildfires in Thailand. Soil water deficits increase dry conditions, resulting in more intense and longer burning wildfires. The temperature vegetation dryness index (TVDI) and the normalized difference drought index (NDDI) were used to estimate soil moisture during the dry season to explore its use for wildfire risk assessment. The results reveal that the normalized difference wet index (NDWI) and land surface temperature (LST) can be used for TVDI calculation. Scatter plots of both NDWI/LST and the normalized difference vegetation index (NDVI)/LST exhibit the triangular shape typical for the theoretical TVDI. However, the NDWI is more significantly correlated to LST than the NDVI. Linear regression analysis, carried out to extract the maximum and minimum LSTs (LST_{max} , LST_{min}), indicate that LST_{max} and LST_{min} delineated by the NDWI better fulfill the collinearity requirement than those defined by the NDVI. Accordingly, the NDWI-LST relationship is better suited to calculate the TVDI. This modified index, called $TVDI_{NDWI-LST}$, was applied together with the NDDI to establish a regression model for soil moisture estimates. The soil moisture model fulfills statistical requirements by achieving 76.65% consistency with the actual soil moisture and estimated soil moisture generated by our model. The relationship between soil moisture estimated from our model and leaf fuel moisture indicates that soil moisture can be used as a complementary dataset to assess wildfire risk, because soil moisture and fuel moisture content (FMC) show the same or similar behavior under dry conditions.

Keywords: wildfire, soil moisture, fuel moisture content, vegetation index, Landsat 8, northern Thailand

1. Introduction

Severely dry climate plays an important role in the occurrence of wildfires. In Thailand, forest wildfires are particularly prevalent during the dry season and are especially damaging because of forest loss and degradation. During the dry season, the number of wildfires in Thai conserved forest areas were 4207, 4982, and 6685 in 2014, 2015, and 2016, respectively (Forest Fire Control Division, 2016). These numbers indicate that the number of wildfires appears to be increasing because Thailand has been experiencing longer dry seasons and under dry conditions, wildfires can ignite easily, as fuel sources are readily available. Fuel availability, which drives wildfire occurrences and directly affects wildfire behavior, depends on fuel characteristics, which are fuel load (influencing fire intensity) and fuel moisture content (influencing both fire ignition and spread). It appears that recurring dry seasons foster fuel availability and reduce fuel moisture content, resulting in potentially more damaging high-intensity fires, which may spread rapidly during extremely dry conditions.

Soil moisture, defined as the volumetric water content of soil (Eller & Denoth, 1996), is an important indicator of dry conditions and is linked to wildfire occurrence. The reduction of water in soil increases dry conditions, resulting in more intense and longer burning fires (Kozłowski & Pallardy, 2002; Chmura et al., 2011). Previous studies pointed out that soil moisture affects wildfire occurrence. For example, Krueger et al. (2015) showed that large growing-season wildfires occurred exclusively under conditions of low soil moisture. Yebra et al. (2013) suggested that improving wildfire assessments involves using soil moisture as a representative for fuel moisture, which is a key factor for ignition and spread of wildfires. Therefore, surface measurements of soil moisture may provide opportunities for improving estimates of fuel moisture (Qi, Dennison, Spencer, & Riano, 2012), because both are physically linked through soil-plant interactions (Hillel, 1998).

Remote sensing techniques have been extensively used for the analysis of soil moisture, and have provided alternative tools for obtaining rapid estimates of soil moisture on large spatial scales (Goward, Xue, & Czajkowski, 2002; Sandholt, Rasmussen, & Andersen, 2002; Ishimura, Shimizu, Rahimzadeh, & Omasa, 2011). Vegetation indices (VIs), which are mathematical combinations of different spectral bands from satellite remotely sensed data, have been utilized to estimate soil moisture (Z. Gao, W. Gao, & Chang, 2011; Chen et al., 2015). The normalized difference vegetation index (NDVI) is the normalized reflectance difference between the near-infrared (NIR) and visible red (R) bands (Rouse, Haas, Deering, Schell, & Harlan, 1974; Tucker, 1979), which measures changes in chlorophyll content. As a result, it is considered a function of vegetation strength, which changes as vegetation interacts with soil moisture. The normalized difference water index (NDWI) is a more recent satellite-derived index from the NIR and short-wave infrared (SWIR) channels that reflects changes in both water content and spongy mesophyll in vegetation canopies (Gao, 1996). This index has been employed for the determination of vegetation water content and stress (Ceccato, Gobron, Flasse, Pinty, & Tarantola, 2002), and is therefore expected to be linked to soil moisture due to its impact on vegetation water stress. Moreover, land surface temperature (LST) can rise rapidly with water stress (Goetz, 1997), which is directly related to soil moisture. Accordingly, LST is also widely used as a soil moisture indicator (Carlson, 2007).

The relationship between VI and LST has been investigated to evaluate evapotranspiration rates. The VI-LST relationship normally shows a negative correlation, resulting in triangular-shaped VI-LST plots at different spatial scales (Nemani, Pierce, Running, & Goward, 1993; Goetz, 1997). Based on the VI-LST correlation, the temperature vegetation dryness index (TVDI), computed from the NDVI-LST relationship has become a widely used dryness index to estimate surface soil moisture (Sandholt, Rasmussen, & Andersen, 2002; Mallick, Bhattacharya, & Patel, 2009; Patel, Anapashsha, Kumar, Saha, & Dadhwal, 2009). For example, Wang, Qu, Zhang, Hao, and Dasgupta (2007) applied NDVI-LST produced from moderate resolution imaging spectroradiometer (MODIS) data to investigate the correlation with soil moisture determined by field measurements. The results revealed that NDVI-LST is strongly correlated with soil moisture and can be used to generate soil moisture estimates. Chen et al. (2015) used the TVDI (NDVI-LST) derived from Landsat-5 TM data to estimate soil moisture and found that the TVDI can reflect the soil moisture status under different tree species. In this study, we propose a new application of the NDWI-LST relationship, which could enhance the efficiency of the TVDI calculation. Additionally, the normalized difference drought index (NDDI), which combines information about both greenness and water obtained from the NDVI and the NDWI (Gu, Brown, Verdin, & Wardlow, 2007), has been applied in numerous studies to evaluate drought and it was found that it is an appropriate indicator for the dryness of a particular area (Renza, Martinez, Arquero, & Sanchez, 2010; Gouveia, Bastos, Trigo, & DaCamara, 2012). The NDDI appears to respond to soil moisture based on drought conditions, and was used in this study to determine soil moisture.

The objectives of this study are to estimate the spatial distribution of soil moisture using VIs based on Landsat 8 OLI/TIRS data and to evaluate the use of soil moisture data for wildfire risk assessment. Specifically, this paper includes: (1) soil moisture estimates for mapping the spatial distribution of soil moisture by combining TVDI and NDDI based on a regression approach. We propose a possible adaptation and application of NDWI and LST for constructing a TVDI based on the similar design of the triangular NDVI-LST space. We then compare the efficiencies of NDVI-LST and NDWI-LST for calculating the TVDI. (2) An investigation of the relationship between estimated soil moisture and fuel moisture measured in the field to assess the suitability of the simulated soil moisture data for wildfire prediction. (3) We hypothesize that (i) the NDWI-LST relationship performs as well as or better than the NDVI-LST relationship and can be applied for calculating TVDI, and (ii) that estimated soil moisture derived from our model is directly related to fuel moisture, influencing wildfire occurrence. In this study, we used the Landsat 8 TIRS and MODIS products for calculating LST and the Landsat 8 OLI product for determining TVDI and NDDI.

This study could also be used as an approach to enhance the efficiency of wildfire assessment using soil moisture as a surrogate for fuel moisture, identifying areas prone to wildfire across different landscapes. Until now, Thailand has not widely applied remote sensing to wildfire management. Using soil moisture measured by remote sensing as a complementary dataset for wildfire management may have the unique potential to predict wildfire danger for Thailand's forest areas and enhance the effectiveness of planning and decision-making in the area of wildfire management.

2. Materials and Methods

2.1 Study Area

Sri Lanna National Park, located in Chiang Mai province in northern Thailand, is the field measurement area for soil moisture (Figure 1). The park consists of a mountain chain, running north to south, with elevations varying from 400 to 1718 meters above sea level. The study mainly focused on 63,965 ha of dipterocarp forest and 20,528 ha of deciduous forest (Department of National Parks, Wildlife and Plant Conservation [DNP], 2003). Wildfires mostly occur during the dry season (from December to April), when trees shed their leaves, and leaf litter quickly accumulates, serving as available fuel to drive wildfires. The mean annual temperature in the study area is 26.7 °C, while the minimum and maximum temperatures of the coldest (January) and hottest months (April) are 11.0 °C and 39.5 °C, respectively (Thai Meteorological Department, 2014). The area receives an average precipitation of 1,156 mm yr⁻¹. August is the month with the highest precipitation of 256.76 mm, which decreases in the dry season and reaches a minimum of 4.10 mm in February (DNP, 2003). Soil properties in the park are closely related to slope; 92.2% of the total forest area is classified as a soil slope complex series, which is found in areas with slopes that exceed 35%. Sandy and sandy loam soils are dominant (DNP, 2003).

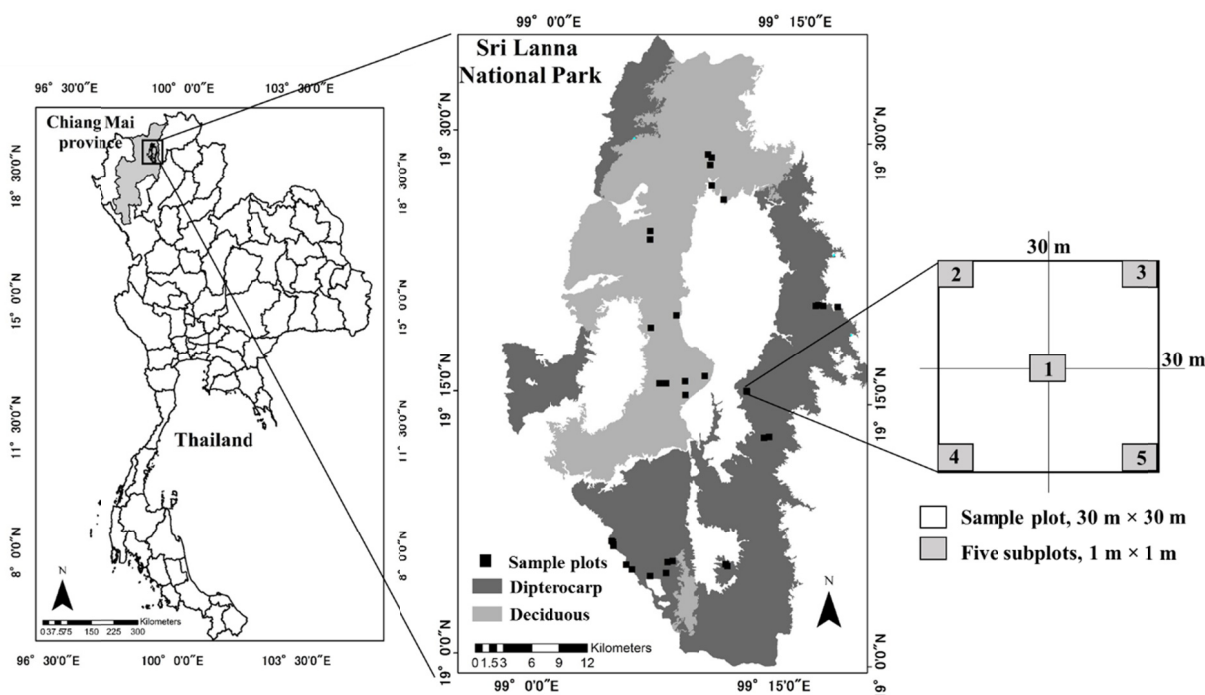


Figure 1. Location map and observation sites in Sri Lanna National Park

2.2 Field Measurements

Thirty-four sample plots with heterogeneous landscape and ecological conditions were selected using a topographic map. A Landsat 8 image provided radiometric and geometric corrections for different slopes, aspects, and forest types. The selected plots were evaluated during the dry season in March 2015. Larger 30 m × 30 m sample areas, corresponding to the spatial resolution of Landsat 8 images (30 m × 30 m pixel size) used for linear regression analysis, were divided into five subplots (1 m × 1 m) for collecting soil samples and fuel or litter from the ground surface.

2.2.1 Gravimetric Soil Moisture Measurements

Soil samples were collected from each of the five 1-m² subplots, which are representative of the soil within each sample plot. The soil samples were taken at a standard depth of 10 cm, because previous studies have indicated that it is feasible to estimate surface (0 to 0.76 cm) soil moisture from visible and NIR reflectance (Kaleita, Tian, & Hirschi, 2005). In addition, VIs show the highest correlation with surface soil moisture at 10 cm depth (Zhang,

Hong, Qin, & Zhu, 2013). Each soil sample was placed in a plastic container and sealed tightly for further laboratory analysis. For the gravimetric analysis of soil moisture, we first weighed the soil samples (wet weight in grams) using a standard laboratory scale and then placed them in a drying oven at 105 °C for 48 hours (Gardner, 1986). After drying, we weighed the dried soil samples (dry weight in grams). The percentage of gravimetric soil moisture was calculated using Equation 1:

$$\text{Soil moisture} = \frac{\text{wet weight} - \text{dry weight}}{\text{dry weight}} \times 100\% \quad (1)$$

Five soil moisture measurements from each of the five subplots within each sample plot were averaged to obtain representative soil moisture for each 30-m² site, corresponding to the spatial resolution of the Landsat 8 images. The averaged soil moisture data from 34 sample plots were used for both training (80%) and validation (20%) data.

2.2.2 Leaf Fuel Moisture Measurements

Leaf fuel was collected for fuel moisture measurements, which were used for analyzing the relationship with simulated soil moisture. We specifically focused on dead leaves on the ground surface, because those represent the largest fuel component. A small sample of leaf litter was randomly collected from each 1-m² subplot and then placed into a sealed envelope for further laboratory analysis. In the laboratory, leaf litter samples were weighed and oven-dried at 80 °C for 48 hours, then weighed again to calculate the fuel moisture content (FMC) in percent following the procedure described by Desbois, Deshayes and Beudoin (1997). The most common FMC calculation is the ratio of water to dry weight as expressed by Equation 2. The FMC values for the five subplots were averaged to obtain a representative FMC for each 30-m² sample plot.

$$\text{FMC} = \frac{\text{wet weight} - \text{dry weight}}{\text{dry weight}} \times 100\% \quad (2)$$

2.3 Remotely Sensed Data and Preprocessing

We used cloud-free Landsat 8 OLI/TIRS and MODIS eight-day composite LST datasets at a spatial resolution of 30 m and 1000 m, respectively, as primary data (Table 1). Estimates of soil moisture require: (i) Landsat 8 images to extract the TVDI and NDDI, and (ii) MODIS eight-day composite LST and Landsat 8 thermal infrared (TIR) data to produce the LST. Landsat 8 datasets used are the L1G level product and were geographically corrected and clipped based on the study area's boundary. The MODIS data were (i) projected to UTM Zone 47N with the WGS84 datum, (ii) clipped based on the study area's boundary, and (iii) co-registered to Landsat 8 images to reduce potential geometric errors.

Table 1. Selected Landsat 8 and MODIS images for dry season

Season	Parameter	Landsat 8		MODIS eight-day composite	
		Acquisition date	Spectral band	Acquisition date	Product
Dry	TVDI, NDDI	19 Feb 2015	Visible, NIR, SWIR	–	–
Dry	LST	19 Feb 2015	TIR (band 10)	18-25 Feb 2015	MOD11A2

2.4 Soil Moisture Estimates

2.4.1 Calculation of the TVDI

The LST is the temperature of the Earth's surface as derived from remotely sensed thermal infrared data (Weng, Fu, & Gao, 2014). It depends on the albedo, vegetation cover, and soil moisture. The Landsat 8 LST was computed by fusing images of MODIS LST and Landsat 8 brightness temperature (T_b), provided by Hazaymeh and Hassan (2015). Generating Landsat 8 LST was based on the linear relationship between MODIS LST and Landsat 8 T_b, which were obtained almost simultaneously and under similar atmospheric conditions.

A scatter plot of remotely sensed LST and VI often results in a triangular shape (Price, 1990; Carlson, Gillies, & Perry, 1994) and the “dry” and “wet” edges of the triangle can be used to obtain information on soil moisture content. Figure 2 shows the conceptual TVDI based on the NDVI-LST triangle, where LST is plotted as a function of NDVI. The linear combination of NDVI-LST typically shows a strongly negative relationship and the TVDI can be estimated from the dry and wet edges of the triangle.

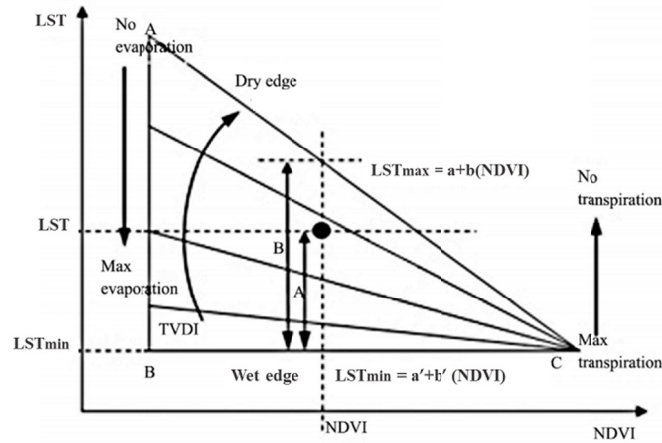


Figure 2. Simplified presentation of TVDI based on the triangular shape of the NDVI-LST relationship (adapted from Sandholt, Rasmussen, & Andersen, 2002)

In the feature space, TVDI is computed based on information about the wet edge representing the minimum LST (LST_{min} , maximum evapotranspiration and thereby, unlimited water access) as a straight line parallel to the NDVI axis. The dry edge, representing the maximum LST (LST_{max} , limited water availability) is linearly correlated with NDVI. Therefore, the TVDI is related to the soil moisture status in that high values indicate dry conditions and low values indicate moist conditions. In this study, the correlations of both NDVI and NDWI to the LST were observed. The TVDI for each pixel can be defined using Equation 3:

$$TVDI = \frac{LST - LST_{min}}{LST_{max} - LST_{min}} \tag{3}$$

Where, LST is the LST (°C) at a given NDVI and NDWI value, LST_{min} is the minimum LST (°C) based on the NDVI and NDWI values along the wet edge, and LST_{max} is the maximum LST (°C) based on the NDVI and NDWI values along the dry edge.

To calculate LST_{max} (dry edge) and LST_{min} (wet edge), we created scatter plots for each NDVI-LST and NDWI-LST pair. Linear regression was applied to scatter plots of the resulting LST_{max} and LST_{min} based on the upper and lower boundary lines of the scatter plots. Positive NDVI and NDWI values were ranked from 0 to 1 and divided into units of 0.01, 0.015, 0.02, 0.025, ... 1. Then, each of the individual values of the scaled NDVI and NDWI were paired with a corresponding LST such as $NDVI_1, LST_{max1}$ and $NDVI_1, LST_{min1}$ or $NDWI_1, LST_{max1}$ and $NDWI_1, LST_{min1}$. Finally, we employed a linear regression approach to fit the point pairs for generating LST_{max} and LST_{min} :

$$LST_{max} = a + b (VI) \tag{4}$$

$$LST_{min} = a' + b' (VI) \tag{5}$$

Where, a and b are regression coefficients of LST_{max} , a' and b' are regression coefficients of LST_{min} , and VI represents the NDVI and NDWI values. The NDVI is a normalized ratio of the NIR and R reflectance (Tucker, 1979) as described in Equation 6. The NDWI is calculated from NIR and SWIR reflectance (Gao, 1996) as shown in Equation 7:

$$NDVI = \frac{NIR - RED}{NIR + RED} \tag{6}$$

$$NDWI = \frac{NIR - SWIR}{NIR + SWIR} \tag{7}$$

We investigated the NDVI and the NDWI performance and selected the index showing the strongest correlation with LST based on the adjusted R-squared ($adj-R^2$) of LST_{max} and LST_{min} . The best relationship of the index and LST was later used for TVDI calculation following Equation 3.

2.4.2 Calculation of the NDDI

The NDDI was computed from the NDVI and NDWI values according to the definition proposed by Gu, Brown, Verdin, and Wardlow (2007). The combination of information about both vegetation (NDVI) and water (NDWI) conditions can be used to determine vegetation drought conditions, which reflect the effects of soil moisture. Due to the variation of the NDVI and NDWI within a range from -1 to +1, these values were converted to 8 bits (0-255) for the calculation of the NDDI, which ranges between -1 and +1. Higher NDDI values indicate more severe drought and lower soil moisture. The NDDI is computed as:

$$NDDI = \frac{NDVI - NDWI}{NDVI + NDWI} \quad (8)$$

2.4.3 Soil Moisture Model and Validation

We established a soil moisture estimation model based on a collection of field sampling and remote sensing data. A stepwise multiple regression approach was used to assess the relationship between field soil moisture data and remote sensing data, i.e., TVDI and NDDI were used as independent variables. The model can be computed by a regression formula as follows:

$$\text{Estimated soil moisture} = a + b(TVDI) + b'(NDDI) \quad (9)$$

Where, the estimated soil moisture is given as a percentage (%), and a , b , and b' are the coefficients of the regression lines of the TVDI and NDDI.

The model was validated by ground and remote sensing data. We used the actual soil moisture from the field measurements to evaluate the accuracy of the predictive model by statistical inference: (i) adj-R², (ii) root mean squared error (RMSE), (iii) absolute average difference (AAD), and (iv) the precision of the model. The precision (%) of the model is calculated as follows:

$$\text{Precision} = \sqrt{\frac{\sum[(Y_i - Y'_i) / Y'_i]^2}{N}} \times 100\% \quad (10)$$

Where, Y_i is the actual soil moisture of the field samples (%), Y'_i is the estimated soil moisture from remotely sensed data (%), and N is the sample size.

Finally, the validated model was applied to a Landsat 8 image acquired on 19 February 2015 in Sri Lanna National Park (dipterocarp and deciduous forests) in order to estimate and map the spatial soil moisture distribution during the dry season.

2.5 Analysis of the Relationship between Estimated Soil Moisture and Leaf Fuel Moisture

To investigate the relationship between soil moisture estimated from our model and FMC, we performed a correlation analysis using the Pearson correlation and linear regression methods. Estimated soil moisture was extracted from the model at the same locations as were used to measure leaf fuel moisture in the field to determine correlation. We then explored the possibility of applying estimated soil moisture from our model to the prediction of wildfire occurrences.

3. Results and Discussion

Scatter plots of the relationships between NDVI-LST and NDWI-LST are shown in Figure 3. Compared to the NDVI-LST plot, the NDWI-LST relationship shows a clearer triangular shape, following the theoretical triangle of the TVDI. We determined LST_{max} (dry edge) and LST_{min} (wet edge) to highlight linear trends. A comparison of pixels representing LST_{max} and LST_{min} extracted from the NDVI-LST and the NDWI-LST plots indicates a stronger relationship between these pixels in the NDWI-LST space. Based on Figure 3, the LST_{max}, representing the dry edge, shows a strong negative correlation between the NDWI and LST (adj-R² = 0.84, p-value < 0.01), and the LST_{min}, representing the wet edge, shows a negative correlation between the NDWI and LST with adj-R² = 0.63 at a significant level for p < 0.01. In contrast, NDVI has a lower correlation with LST, with LST_{max} at adj-R² = 0.62 (p-value > 0.05) and LST_{min} at adj-R² = 0.47 (p-value < 0.01). The results of the collinearity requirement indicate that the NDWI has a stronger negative correlation with the LST than the NDVI, which is why the NDWI was used to calculate TVDI.

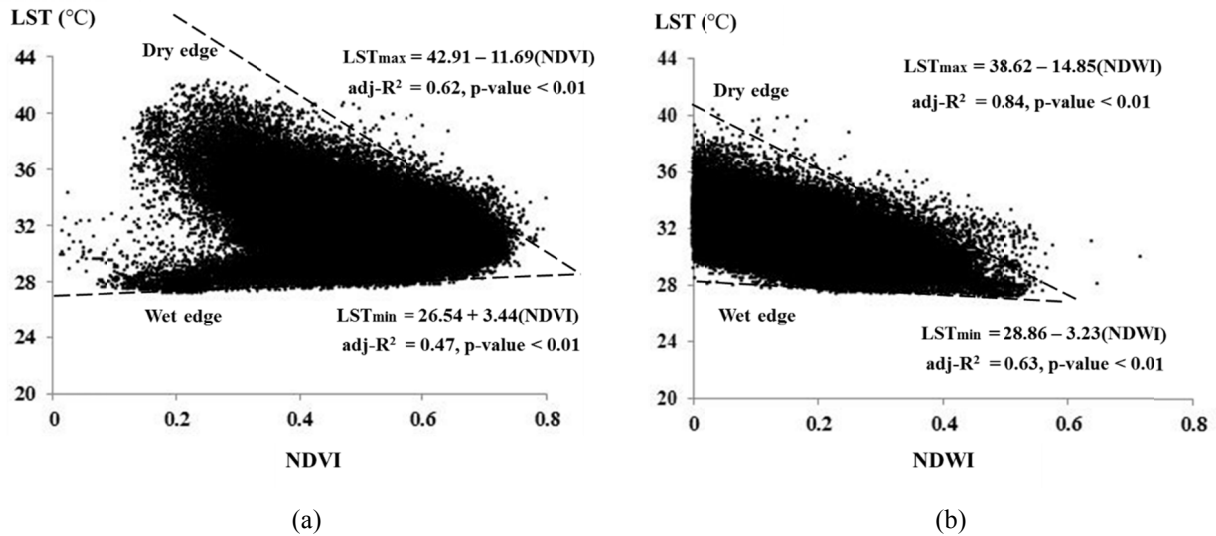


Figure 3. Observed relationships for (a) NDVI-LST and (b) NDWI-LST, based on the conceptual TVDI model

The reason for the better correlation between the NDWI and LST might be that LST is more strongly related to the water content of vegetation (captured by NDWI) than to the chlorophyll content (captured by NDVI). The NDVI measures changes in chlorophyll content (absorption of visible red radiation) and in the leaf spongy mesophyll (reflection of NIR radiation) within the vegetation canopy. Consequently, the NDVI has a limited capability for retrieving vegetation water content information, as it provides information on vegetation greenness (chlorophyll), which is not directly and uniformly related to the quantity of water in the vegetation (Ceccato, Gobron, Flasse, Pinty, & Tarantola, 2002). A change in chlorophyll content detected using the NDVI does not imply a direct change in leaf water content. Conversely, the NDWI is sensitive to changes in leaf water content because the green vegetation spectra in the SWIR region are dominated by water absorption.

The water content in leaves is directly affected by temperature conditions, especially high temperatures. As temperature increases, evaporation from leaves is higher, which affects the water content of the leaves. Evaporation within leaves also causes an increase in heat, and the leaf temperature rises relative to the air temperature or LST. Therefore, NDWI is more sensitive to LST, resulting in a stronger negative correlation with LST. Gu, Brown, Verdin, and Wardlow (2007) found that NDWI values exhibited a quicker response to drought conditions when compared to NDVI values. This is because the NDWI is constructed from the SWIR, which is more sensitive to moisture than other spectra. As a result, the NDWI shows a better correlation with LST and follows more closely the conceptual TVDI model. This result supports our hypothesis that the relationship between the NDWI and LST can be used to improve the calculation of the TVDI.

A TVDI map of the study area extracted from LST_{max} and LST_{min} based on the strong NDWI-LST relationship is shown in Figure 4a, while a NDDI map computed from the NDVI and the NDWI is shown in Figure 4b. Both maps, which show drought conditions during the dry season, can reflect the degree of soil moisture because drought influences the soil moisture status. Extreme drought results in lower soil moisture content. Therefore, both VIs can be used as predictor variables to estimate soil moisture.

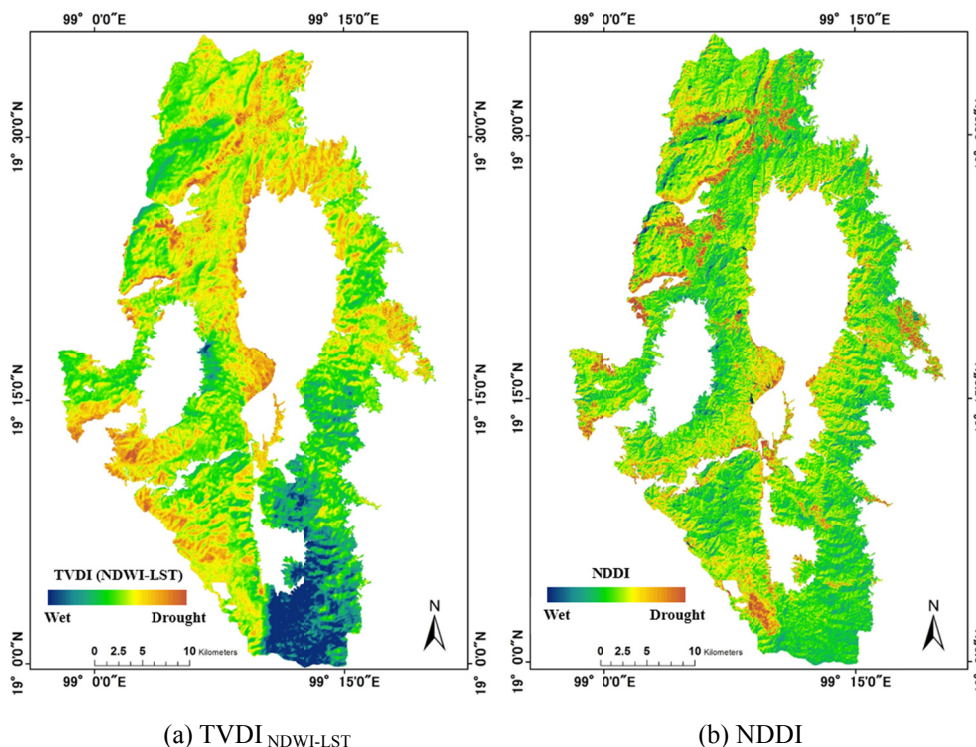


Figure 4. Extraction of a Landsat 8 image from 19 February 2015 for (a) TVDI_{NDWI-LST} and (b) NDDI

Linear regression models for soil moisture estimation shown in Table 2 were calculated using the modified TVDI_{NDWI-LST} and the NDDI as dependent variables, and field-measured soil moisture content as the independent variable. The model constructed from both indices has the strongest response to the actual soil moisture and likely has a greater ability to accurately estimate soil moisture, based on its high adj-R² (0.89, p-value < 0.01) and low RMSE (0.87%) for actual versus estimated soil moisture. In contrast, the model that only uses TVDI_{NDWI-LST} has a lower adj-R² (0.72, p-value < 0.01) and a higher RMSE value of 1.39 %. Similarly, the model that only uses the NDDI shows the weakest correlation with an adj-R² of 0.52 (p-value < 0.01) and the highest RMSE of 1.82%. Thus, the soil moisture model using both the TVDI_{NDWI-LST} and the NDDI fulfills the collinearity requirements with an increase in the adj-R² and a reduced RMSE, which can enhance the efficiency of soil moisture estimation.

Table 2. Comparison of statistical soil moisture models

Predictor variable	Soil moisture model (%)	N	adj-R ²	RMSE (%)
TVDI _{NDWI-LST}	10.67 – 12.24(TVDI _{NDWI-LST})	27	0.72*	1.39
NDDI	13.93 – 35.44(NDDI)	27	0.52*	1.82
TVDI _{NDWI-LST} , NDDI	14.32 – 9.45(TVDI _{NDWI-LST}) – 21.78(NDDI)	27	0.89*	0.87

Note. * is significant at the 0.01 level.

The best model, developed from the combination of the modified TVDI_{NDWI-LST} and the NDDI, was tested for accuracy with regard to field-measured soil moisture, resulting in the statistical parameters shown in Table 3. The model fulfills the statistical requirements. We found a high adj-R² of 0.75 with a p-value of < 0.01. We obtained low RMSE and AAD values of 1.22% and 1.06% between the actual and estimated soil moisture, respectively. In addition, the model precision was found it to be 76.65% consistent with the actual and estimated soil moisture. These statistical tests demonstrate that the model generated from the modified TVDI_{NDWI-LST} and the NDDI can provide reliable estimates of soil moisture.

Table 3. Statistical validation between the actual and soil moisture estimated from the model

Soil moisture model (%)	N	adj-R ²	RMSE (%)	AAD (%)	Precision (%)
14.32 – 9.45(TVDI _{NDWI-LST}) – 21.78(NDDI)	7	0.75*	1.22	1.06	76.65

Note. * is significant at the 0.01 level.

These results demonstrate that the efficacy of soil moisture estimation can be greatly enhanced using TVDI (modified from NDWI-LST) and NDDI as dependent variables, because both VIs show a strong correlation with soil moisture measured in the field. The reason for this strong correlation is the causal relationship between variations in soil moisture and changes in vegetation; consequently, soil moisture deficits are ultimately tied to drought stress in plants (Gu et al., 2008), which is captured by both the TVDI and NDDI. Based on these results, we applied the model to a Landsat 8 image taken during the dry season to estimate soil moisture (Figure 5). The spatial distribution map shows that the percentage of soil moisture in Sri Lanna National Park is quite low during the dry season at around 0.001% to 31.1%, with a mean value of 15.49%. The degree of estimated soil moisture can indicate drought conditions, which in turn influence the occurrence of wildfires. Areas with lower soil moisture and resulting lower fuel moisture, which influences fire ignition and spread, are more prone to wildfire occurrence.

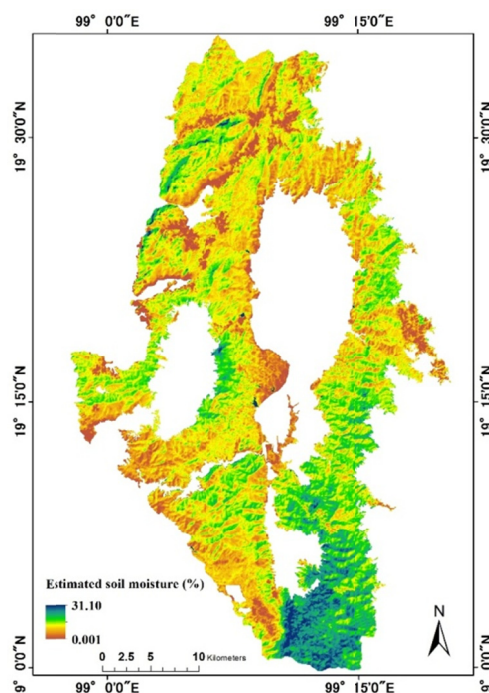


Figure 5. Spatial distribution of soil moisture derived from the model generated by the modified TVDI_{NDWI-LST} and the NDDI in Sri Lanna National Park during the dry season on 19 February 2015

We also investigated the correlation between the estimated soil moisture and leaf fuel moisture determined in the field (Figure 6). Pearson's correlation reveals that leaf fuel moisture shows a statistically significant positive correlation to the estimated soil moisture (Pearson's correlation coefficient = 0.67, p-value < 0.01). Larger values of estimated soil moisture tend to be associated with larger values of leaf fuel moisture. This implies that leaf fuel moisture has a tendency to increase when estimated soil moisture increases and vice versa. The statistical tests also support our hypothesis that the estimated soil moisture is directly related to FMC.

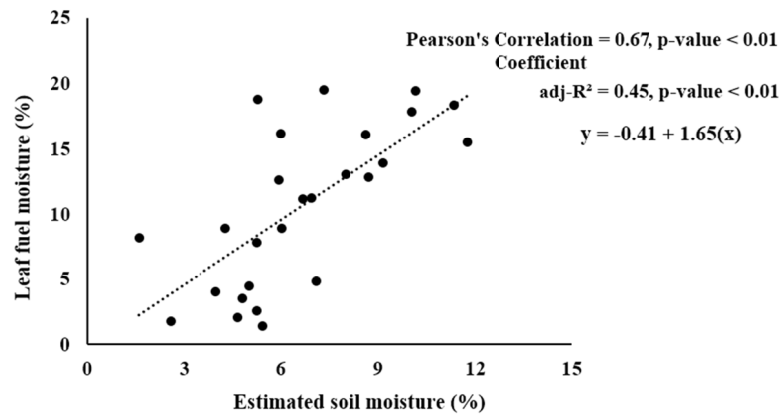


Figure 6. Scatter plot of leaf fuel moisture measured in the field and estimated soil moisture

Moreover, a median adj-R² of 0.45 with a p-value of < 0.01 as shown in Figure 6 indicates that estimated soil moisture is a significant variable for predicting leaf fuel moisture. This suggests that soil moisture is a factor that influences FMC since soil moisture condition affects fuel moisture levels which are directly related to wildfire occurrence. At high temperatures during the dry season, soil moisture and FMC are positively correlated, because high temperatures result in low soil moisture, which in turn leads to low FMC. As a result, we can use soil moisture to assess wildfire risks by exploiting the relationship between soil moisture and FMC. When FMC is high, fires do not readily ignite, because heat energy has to be used to evaporate water from plant material before it can burn. During the combustion of the above ground plant material and surface organic layers, the heat energy created is then transferred in the soil (DeBano, Neary, & Ffolliott, 1998). Thus, fuel load with low moisture can transfer more heat into the soil during the combustion of fuel. Soils with higher moisture content tend to absorb more heat energy (DeBano, Neary, & Ffolliott, 1998, 2005); as a result, the intensity of the fire is reduced. In cases where both the FMC and soil moisture are low wildfires will start much easily and spread rapidly resulting in uncontrollable fire condition.

Based on the result, mapping of estimated soil moisture can be used to investigate wildfire risk in large areas. Additionally, soil moisture can give an insight on the dryness of the fuel, which is a crucial parameter for wildfire risk. Therefore, to reduce wildfire risk and intensity, soil moisture should be considered as another indicator for monitoring wildfire prone areas. An analysis of soil moisture could considerable enhance wildfire management, thus in our study we highly recommend estimating soil moisture by remotely sensed data to be used as a complementary dataset for wildlife management in terms of risks and danger assessment.

4. Conclusion

The main goal of this study was to estimate the spatial distribution of soil moisture using TVDI and NDDI derived from Landsat 8 OLI/TIRS data for wildfire risk assessment. Results reveal that an accurate estimate of TVDI can be obtained from the relationship between NDWI, which is more significantly correlated to LST than the NDVI, and LST. This modified TVDI_{NDWI-LST} can be used together with the NDDI to enhance the efficacy of soil moisture estimation. A scatter plot of NDWI-LST shows a linear relationship and is a good match with the theoretical concept of the TVDI, which is characterized by the triangular shape of the NDVI-LST relationship. The good correlation between NDWI and LST fulfills the collinearity requirements for extracting LST_{max} and LST_{min}; consequently, the NDWI-LST relationship provides a better estimate of the TVDI than the NDVI-LST relationship.

The soil moisture model generated from a combination of the modified TVDI_{NDWI-LST} and NDDI can improve the accuracy of soil moisture estimates. The accuracy of the model was tested using statistical metrics, and was found to be more than 76% consistent with actual soil moisture and estimated soil moisture derived from our model. We further explored the relationship between estimated soil moisture and wildfire risk by investigating the correlation between estimated soil moisture and leaf fuel moisture measured in the field. Results show that estimated soil moisture is positively correlated to leaf fuel moisture with a Pearson's correlation coefficient of 0.67 (p-value < 0.01). This relationship demonstrates that wildfire-prone areas, which are characterized by low FMC, can be identified through soil moisture estimates, because both soil moisture and FMS show the same or similar behavior under conditions of high temperatures during the dry season.

The model allows to remotely determine the spatial distribution of soil moisture as a complementary dataset for identifying wildfire-prone areas, which is a fundamental step toward involving soil moisture in the assessment of wildfire risk. We therefore recommend soil moisture estimation by remotely sensed model as another indicator for monitoring wildfire risks and intensity. Furthermore, the demonstrated NDWI-LST relationship provides another option for researchers studying soil moisture when the established TVDI based on the NDVI-LST relationship is insufficient. Future studies should address soil moisture as one of the factors used for enhancing estimates of FMC, as soil moisture is shown to be correlated with FMC.

Acknowledgements

The financial supports and the GIS based thematic maps were provided by Department of National Parks, Wildlife and Plant Conservation, Thailand. We truly thank Mr. Yossawat Thiansawat the Sri Lanna National Park superintendent for the field data collection.

References

- Carlson, T. N. (2007). An overview of the triangle method for estimating surface evapotranspiration and soil moisture from satellite imagery. *Sensors*, 7, 1612-1629. <http://dx.doi.org/10.3390/s7081612>
- Carlson, T. N., Gillies, R. R., & Perry, E. M. (1994). A method to make use of thermal infrared temperature and NDVI measurements to infer surface soil water content and fractional vegetation cover. *Remote Sensing Reviews*, 9, 161-173.
- Ceccato, P., Gobron, N., Flasse, S., Pinty, B., & Tarantola, S. (2002). Designing a spectral index to estimate vegetation water content from remote sensing data: Part 1 Theoretical approach. *Remote Sensing of Environment*, 82, 188-197. [http://dx.doi.org/10.1016/S0034-4257\(02\)00037-8](http://dx.doi.org/10.1016/S0034-4257(02)00037-8)
- Chen, S., Wen, Z., Jiang, H., Zhao, Q., Zhang, X., & Chen, Y. (2015). Temperature vegetation dryness index estimation of soil Moisture under different tree species. *Sustainability*, 7, 11401-11417. <http://dx.doi.org/10.3390/su70911401>
- Chmura, D. J., Anderson, P. D., Howe, G. T., Harrington, C. A., Halofsky, J. E., Peterson, D. L., ... Clair, J. B. St. (2011). Forest responses to climate change in the northwestern United States: Ecophysiological foundations for adaptive management. *Forest Ecology and Management*, 261, 1121-1142. <http://dx.doi.org/10.1016/j.foreco.2010.12.040>
- DeBano, L. F., Neary, D. G., & Ffolliott, P. F. (1998). *Fire's effects on ecosystems*. New York, USA: John Wiley & Sons Inc.
- DeBano, L. F., Neary, D. G., & Ffolliott, P. F. (2005). Soil physical properties. In D. G. Neary, K. C. Ryan, & L. F. DeBano (Eds.), *Wildland fire in ecosystems effects of fire on soil and water* (pp. 21-55). USA: USDA Forest Service Gen. Tech. Rep.
- Department of National Parks, Wildlife and Plant Conservation (DNP). (2003). *Sri Lanna National Park's Area Management Master Plan*. Ministry of Natural Resources and Environment, Thailand.
- Desbois, N., Deshayes, M., & Beudoin, A. (1997). Protocol for fuel moisture content measurements. In E. Chuvieco (Ed.), *a review of remote sensing methods for the study of large wildland fires* (pp. 61-72). Spain: Universidad de Alcalá: Alcalá de Henares, Departamento de Geografía.
- Eller, H., & Denoth, A. A. (1996). Capacitive soil moisture sensor. *Journal of Hydrology*, 185, 137-146.
- Forest Fire Control Division. (2016). *Statistics of fire*. Thailand: Department of national parks, wildlife and Plant conservation. Retrieved from <http://www.dnp.go.th/forestfire/2546/firestatistic%20Th.htm>
- Gao, B. (1996). NDWI—A normalized difference water index for remote sensing of vegetation liquid water from space. *Remote Sensing of Environment*, 58, 257-266.
- Gao, Z., Gao, W., & Chang, N. B. (2011). Integrating temperature vegetation dryness index (TVDI) and regional water stress index (RWSI) for drought assessment with the aid of LANDSAT TM/ETM+ images. *International Journal of Applied Earth Observation and Geoinformation*, 13, 495-503. <http://dx.doi.org/10.1016/j.jag.2010.10.005>
- Gardner, W. H. (1986). Water content. In A. Klute (Ed.), *Methods of Soil Analysis. Part 1. Physical and Mineralogical Methods* (2nd ed.). Madison, Wisconsin, USA: Soil Science Society of America, Inc.

- Goetz, S. J. (1997). Multisensor analysis of NDVI, surface temperature and biophysical variables at a mixed grassland site. *International Journal of Remote Sensing*, 18(1), 71-94. <http://dx.doi.org/10.1080/014311697219286>
- Gouveia, C. M., Bastos, A., Trigo, R. M., & Daamaral, C. C. (2012). Drought impacts on vegetation in the pre- and post-fire events over Iberian Peninsula. *Natural Hazards and Earth System Sciences*, 12, 3123-3137.
- Goward, S. N., Xue, Y. K., & Czajkowski, K. P. (2002). Evaluating land surface moisture conditions from the remotely sensed temperature/vegetation index measurements: An exploration with the simplified simple biosphere model. *Remote Sensing of Environment*, 79(2-3), 225-242. [http://dx.doi.org/10.1016/S0034-4257\(01\)00275-9](http://dx.doi.org/10.1016/S0034-4257(01)00275-9)
- Gu, Y., Brown, J. F., Verdin, J. P., & Wardlow, B. (2007). A five year Analysis of MODIS NDVI and NDWI for grassland drought assessment over the central great plains of United States. *Geophysical Research Letters*, 34(6). <http://dx.doi.org/10.1029/2006GL029127>
- Gu, Y., Hunt, E., Wardlow, B., Basara, J. B., Brown, J. F., & Verdin J. P. (2008). Evaluation of MODIS NDVI and NDWI for vegetation drought monitoring using Oklahoma Mesonet soil moisture data. *Geophysical Research Letters*, 35, 1-5. <http://dx.doi.org/10.1029/2008GL035772>
- Hazaymeh, K., & Hassan, Q. K. (2015). Fusion of MODIS and Landsat-8 Surface Temperature Images: A New Approach. *PloS One* 2015, 10(3), e0117755. <http://dx.doi.org/10.1371/journal.pone.0117755>
- Hillel, D. (1998). *Environmental soil physics* (1st ed.). San Diego, California, USA: Academic Press.
- Ishimura, A., Shimizu, Y., Rahimzadeh, B. P., & Omasa, K. (2011). Remote sensing of Japanese beech forest decline using an improved Temperature Vegetation Dryness Index (iTVDI). *iForest-Biogeosciences and Forestry*, 4, 195-199. <http://dx.doi.org/10.3832/ifor0592-004>
- Kaleita, A. L., Tian, L. F., & Hirschi, M. C. (2005). Relationship between soil moisture content and soil surface reflectance. *American Society of Agricultural Engineers*, 48(5), 1979-1986. <http://dx.doi.org/10.13031/2013.19990>
- Kozlowski, T. T., & Pallardy, S. G. (2002). Acclimation and adaptive responses of woody plants to environmental stresses. *The Botanical Review*, 68(2), 270-334.
- Krueger, E. S., Ochsner, T. E., Engle, D. M., Carlson, J. D., Twidwell, D., & Fuhlendorf, S. D. (2015). Soil moisture affects growing-season wildfire size in the Southern Great Plains. *Soil Science Society of America Journal*, 79, 1567-1576.
- Mallick, K., Bhattacharya, B. K., & Patel, N. K. (2009). Estimating volumetric surface moisture content for cropped soils using a soil wetness index based on surface temperature and NDVI. *Agricultural and Forest Meteorology*, 149, 1327-1342. <http://dx.doi.org/10.1016/j.agrformet.2009.03.004>
- Nemani, R., Pierce, L., Running, S., & Goward, S. (1993). Developing satellite-derived estimates of surface moisture status. *Journal of Applied Meteorology*, 32, 548-557.
- Patel, N. R., Anapashsha, R., Kumar, S., Saha, S. K., & Dadhwal, V. K. (2009). Assessing potential of MODIS derived temperature/vegetation condition index (TVDI) to infer soil moisture status. *International Journal of Remote Sensing*, 30, 23-39. <http://dx.doi.org/10.1080/01431160802108497>
- Price, J. C. (1990). Using spatial context in satellite data to infer regional scale evapotranspiration. *IEEE Transactions on Geoscience and Remote Sensing*, 28, 940-948.
- Qi, Y., Dennison, P. E., Spencer, J., & Riaño, D. (2012). Monitoring live fuel moisture using soil moisture and remote sensing proxies. *Fire Ecology*, 8, 71-87. <http://dx.doi.org/10.4996/fireecology.0803071>
- Renza, D., Martinez, E., Arquero, A., & Sanchez, J. (2010). Drought estimation maps by means of multirate Landsat fused images. *Remote Sensing for Science, Education, and Natural and Cultural Heritage*, 775-782.
- Rouse, J. W., Haas, H. R., Deering, D. W., Schell, J. A., & Harlan, J. C. (1974). *Monitoring the vernal advancement and retrogradation (green wave effect) of natural vegetation*. NASA/GSFC Type III Final Report, Greenbelt, Maryland, USA. Retrieved from <http://ntrs.nasa.gov/archive/nasa/casi.ntrs.nasa.gov/19740004927.pdf>

- Sandholt, I., Rasmussen, K., & Andersen, J. (2002). A simple interpretation of the surface temperature/vegetation index space for assessment of surface moisture status. *Remote Sensing of Environment*, 79, 213-224. [http://dx.doi.org/10.1016/S0034-4257\(01\)00274-7](http://dx.doi.org/10.1016/S0034-4257(01)00274-7)
- Thai Meteorological Department. (2014). *Climatological data for the year 2014 (Chiang Mai)*. Northern Meteorological Center, Chiang Mai, Thailand.
- Tucker, C. J. (1979). Red and photographic infrared linear combinations for monitoring vegetation. *Remote Sensing of Environment*, 8, 127-150. Retrieved from <http://ntrs.nasa.gov/archive/nasa/casi.ntrs.nasa.gov/19780024582.pdf>
- Wang, L., Qu, J. J., Zhang, S., Hao, X., & Dasgupta, S. (2007). Soil moisture estimation using MODIS and ground measurements in eastern China. *International Journal of Remote Sensing*, 28(6), 1413-1418. <http://dx.doi.org/10.1080/01431160601075525>
- Weng, Q., Fu, P., & Gao, F. (2014). Generating daily land surface temperature at Landsat resolution by fusing Landsat and MODIS data. *Remote Sensing of Environment*, 145, 55-67. <http://dx.doi.org/10.1016/j.rse.2014.02.003>
- Yebra, M., Dennison, P. E., Chuvieco, E., Riano, D., Zylstra, P., Hunt Jr., E. R., ... Jurdao, S. (2013). A global review of remote sensing of live fuel moisture content for fire danger assessment: Moving towards operational products. *Remote Sensing of Environment*, 136, 455-469. <http://dx.doi.org/10.1016/j.rse.2013.05.029>
- Zhang, N., Hong, Y., Qin, Q., & Zhu, L. (2013). Evaluation of the Visible and Shortwave Infrared Drought Index in China. *International Journal of Disaster Risk Science*, 4(2), 68-76. <http://dx.doi.org/10.1007/s13753-013-0008-8>

Copyrights

Copyright for this article is retained by the author(s), with first publication rights granted to the journal.

This is an open-access article distributed under the terms and conditions of the Creative Commons Attribution license (<http://creativecommons.org/licenses/by/4.0/>).